Cu_2O Island Shape Transition during Cu-Au Alloy Oxidation

G.-W. Zhou,[1] L. Wang,[2] R. C. Birtcher,[1] P. M. Baldo,[1] J. E. Pearson,[1] J. C. Yang,[2] and J. A. Eastman[1,*]

[1]*Materials Science Division, Argonne National Laboratory, Argonne, Illinois 60439, USA*

[2]*Materials Science and Engineering Department, University of Pittsburgh, Pittsburgh, Pennsylvania 15261, USA*

(Received 9 February 2006; published 9 June 2006)

In situ transmission electron microscopy observations of the oxidation of (001) Cu-Au alloys indicate that the Cu_2O islands that form undergo a remarkable transformation from an initially compact morphology to a dendritic structure as growth proceeds. Correspondingly, the surface composition becomes nonuniform and the fractal dimension associated with the islands evolves from 2.0 to a stable value of 1.87, indicating a transition in the rate-limiting mechanism of oxidation from oxygen surface diffusion to diffusion of copper through the increasingly gold-rich regions adjacent to the islands.

DOI: 10.1103/PhysRevLett.96.226108 PACS numbers: 68.35.Fx, 68.37.−d, 68.47.De, 81.65.Mq

The formation of a protective oxide layer on a metal surface requires the rapid formation of a continuous film that impedes further oxidation by requiring bulk diffusion through the oxide. A general strategy for the protection of underlying metals is alloying, which leads to the formation of a protective oxide layer over the alloy surface due to the preferential oxidation of one component of the alloy [1]. Two key factors control protective oxide layer formation: thermodynamic stability and oxide continuity. During the initial stages of oxidation, nuclei of several oxides of the alloy components may form, including rapidly oxidizing elements; however, the protective oxide must be the most thermodynamically stable oxide of the major base alloy components [2]. In order to achieve protective behavior, the oxide layer must be continuous, since the existence of discontinuities in the oxide layer leads to rapid diffusion paths. It is still not generally understood which alloying elements improve the likelihood of forming a protective oxide and which degrade behavior due to complicating thermodynamic and kinetic factors.

Copper and copper alloys have wide industrial application, and therefore are of interest for studies of oxidation mechanisms. Under the conditions used in this study, Cu_2O is the stable oxide that forms on Cu, and the cubic Cu_2O lattice aligns epitaxially with the Cu lattice [3,4]. It has been experimentally demonstrated that the oxidation of copper and many other metals on single crystal surfaces proceeds via random nucleation of oxide nuclei, followed by growth and coalescence that leads eventually to a continuous oxide coating [5–7].

Au does not form a stable oxide under most conditions, and is not soluble in Cu_2O. Therefore, the Cu-Au alloy system is ideal for investigating the effect of alloying on the formation of protective oxide layers, in particular, the effect of a nonoxidizing second element on film continuity. Here we report that alloying copper with gold can have a dramatic effect in controlling the morphology of the oxide islands, which in turn prevents coalescence into a continuous and protective film.

Our experiments were carried out in a modified JEOL 200CX TEM equipped to allow observation of oxidation in controlled $p(O_2)$ [8]. Cu-Au (001) single crystal films with ~1000 Å thickness were grown on irradiated NaCl (001) by sputter deposition. The alloy films were removed from the substrate by flotation in deionized water, washed, and mounted on a specially prepared sample holder that allows for resistive heating. Any native Cu oxide is removed by annealing the films in the TEM under vacuum conditions at ~750 °C [9], resulting in a clean copper surface.

Figure 1 is a bright-field TEM image showing how the morphology of a typical Cu_2O island evolved during oxidation of the (001) surface of Cu 15 at. % Au at 600 °C in 5×10^{-4} Torr oxygen partial pressure [$p(O_2)$]. The selected area electron diffraction patterns reveal that regions far from the reaction front, such as *A*, have the Cu face-centered cubic (fcc) structure as observed prior to oxidation. The diffraction pattern from region *B* indicates that the oxide islands are single crystals that nucleate in an epitaxial orientation relationship with the substrate. The

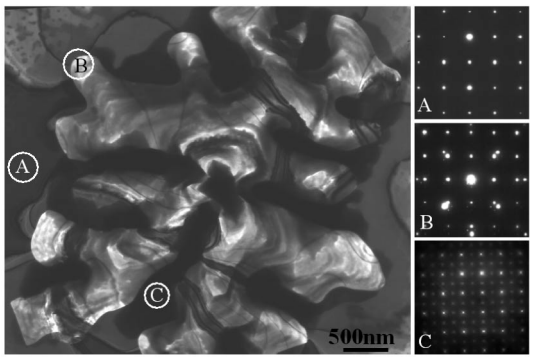

FIG. 1. Typical morphology of dendritic oxide islands obtained during oxidation of Cu 15 at. % Au(100) films at 600 °C in $p(O_2) = 5 \times 10^{-4}$ Torr. The diffraction patterns indicate (a) regions of Cu-Au solubility, (b) epitaxial Cu_2O islands on single-phase Cu-Au alloy regions, and (c) regions where the alloy concentration has evolved as oxidation progresses, such that the $CuAu_3$ ordered phase has formed.

regions with dark contrast such as *C* are Au rich and have the structure of the ordered $CuAu_3$ phase at room temperature. This phase is not observed prior to the onset of oxidation. It is also worth noting that almost no Au accumulation occurs in the alloy film regions in front of the growth tips.

A gradual transition occurs from initially compact island shapes to a dendritic morphology as the islands grow. As seen in Fig. 2, oxide islands nucleate with a square shape and retain this shape during the initial growth. The islands then exhibit a gradual transition to a dendritic shape as growth slows along the normal to the island edges, i.e., along Cu_2O ⟨110⟩ directions, while maintaining a faster growth rate along the directions of the island corners, i.e., along Cu_2O ⟨100⟩ directions. In contrast, the oxide islands formed during oxidation of pure Cu(001) under the same conditions have an initially square shape that transforms to a rectangular morphology as growth proceeds [10]. The contrast features in Figs. 2(a)–2(c) reveal that the alloy film regions adjacent to the island edges become Au rich, while there is almost no excess Au accumulation in the alloy film adjacent to the island corners, as confirmed by energy dispersive x-ray spectroscopy (EDS). Figure 2 clearly reveals that the change in the local growth rate of the island boundary is closely related to this nonuniform partition of Au atoms in the alloy film during the island growth; i.e., the growth rate of the boundary adjacent to the Au-rich zone gradually slows as the local Au concentration increases.

The above observation indicates that the oxidation of Cu-Au alloys is accompanied by the rejection of Au atoms from the growing boundary, leading to Au-rich zones in the alloy adjacent to the metal-oxide interface. The *in situ* TEM observations reveal that the islands initially exhibit parabolic growth behavior, as shown in Figs. 2(a) and 2(d). By applying Fick's diffusion laws and the parabolic growth condition, we can predict the distribution of Cu as a function of distances x, y, and oxidation time t, as follows:

$$N(x,y,t) = N_{\mathrm{Cu}(i)} + (N_{\mathrm{Cu}(b)} - N_{\mathrm{Cu}(i)}) \times \frac{[\mathrm{erf}(\frac{1}{2}\frac{(x+y)}{\sqrt{2Dt}})] - \mathrm{erf}[(\frac{1}{2}\frac{k}{D})^{1/2}]}{1 - \mathrm{erf}[(\frac{1}{2}\frac{k}{D})^{1/2}]}. \quad (1)$$

In Eq. (1), the Cu mole fraction $N_{\mathrm{Cu}(i)}$ at the alloy-oxide interface is determined by the following equation obtained from the moving boundary conditions,

$$(N_{\mathrm{Cu}(b)} - N_{\mathrm{Cu}(i)})/(1 - N_{\mathrm{Cu}(i)}) = F\left[\left(\frac{1}{2}\frac{k}{D}\right)^{1/2}\right], \quad (2)$$

where the auxiliary function $F(u)$ with u as general argument is defined by

$$F(u) = \pi^{1/2} u[1 - \mathrm{erf}(u)]\exp(u^2). \quad (3)$$

The general form of the solution obtained in Eq. (1) is similar to those for problems involving a moving one-dimensional boundary [11].

Figure 2(e) shows the Au composition contour calculated from Eq. (3), where the interdiffusion coefficient D is 7×10^2 nm^2/sec [12] and the determined rate constant k is 550 nm^2/sec. The Au composition contour map in Fig. 2(e) is qualitatively consistent with the EDS measurements and the contrast features seen in Fig. 2(a); i.e., high Au accumulation is indicated in the regions adjacent to the island edges, and low Au accumulation is indicated adjacent to the island corners. This analysis reveals that the nonuniform partition of Au atoms is an intrinsic behavior for the compact growth of the oxide island.

The above analysis assumes that the island growth is controlled by 2D diffusion on the surface of a semi-infinite crystal. Since the surface diffusion rate is much faster than that of bulk transport, and oxide islands on Cu have been observed experimentally to grow more rapidly laterally than normal to the surface [13], contributions from bulk diffusion are expected to have no significant effect on the island growth behavior, and thus have not been included in the analysis. Providing further support that bulk diffusion is not playing a significant role in controlling the oxide morphology, EDS measurements of the oxide regions reveal that the dominant composition changes occur laterally, with no significant Au accumulation beneath the oxide (evidenced by smaller Au concentrations in the Cu_2O-on-alloy regions than in the starting alloy). We expect that similar behavior will occur during oxidation of bulk alloy samples, but this has yet to be demonstrated experimentally.

Tip splitting during the dendritic oxide growth is also observed, as seen in a sequence of images shown in

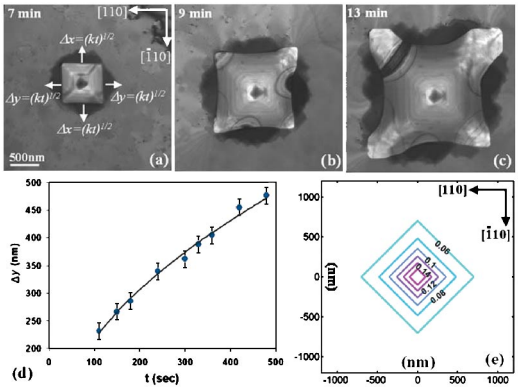

FIG. 2 (color). *In situ* TEM observation of the growth of a Cu_2O island on a Cu 5 at.% Au sample at 600 °C in $p(O_2) = 5 \times 10^{-4}$ Torr. A crossover from (a) an initially compact structure to (b), (c) dendritic growth is observed as time progresses. The total oxidation time is noted on each image; (d) Parabolic growth kinetics are observed prior to the transition to a dendritic morphology; (e) Calculated 2D Au composition contour map for a 7 min oxidation of Cu 5 at.% Au at 600 °C in $p(O_2) = 5 \times 10^{-4}$ Torr (numbers indicate the Au mole fraction). Note that the calculated composition contours are rotated 45° with respect to the oxide island orientation, resulting in minimum Au concentration at island corners.

Fig. 3(a). Due to less Au accumulation at the island corners, the corners grow at a faster rate than the island edges, resulting in a deviation from the initial square morphology. As growth continues, the tip interface gradually becomes flat and forms two new corners because of additional Au segregation and accumulation, as shown in Fig. 3(a) after 12 min of oxidation. Again, there is less Au accumulation in front of the two new corners than along the flat interface, and as a result, the growth front gradually splits again into two new sharp tips. This observation reveals that the tip splitting during the dendritic growth is also an intrinsic behavior associated with segregation and partition of Au atoms.

A useful quantity for characterizing complex growth patterns and establishing a relationship to the growth mechanism is the fractal dimension, D_f. Using the box-counting method [14], we have estimated D_f of the islands at different growth stages, where the box length ε was chosen to be $\varepsilon = 2^n \times$ (pixel size), with $n = 0, \ldots, 9$ for a 1024×1024 pixel image, which yields a ε^{-D_f} scaling behavior. Figure 3(b) shows the evolution of the fractal dimension of the island shown in Fig. 3(a). It shows that the D_f decays monotonically, starting from a large value of 1.93. The fractal dimension corresponding to various morphologies of oxide islands was measured and gives a common value of $\sim 1.87 \pm 0.02$ as shown in Fig. 3(c).

It is quite interesting that the fractal dimension was observed to change as oxide islands grew, evolving from the trivial dimension $D_f = 2$ for a compact island, and stabilizing at $D_f = 1.87$ for islands with a dendritic morphology. We believe that this provides important clues to understanding how the oxidation mechanism evolves with time. In the early stages of metal oxidation under low oxygen pressures and high temperatures, the reaction rate is usually dominated by the capture of oxygen. Indeed, our quantitative analysis of the growth of Cu_2O islands prior to dendrite formation during oxidation of the Cu-Au alloys has revealed that the rate-limiting factor controlling the oxide growth is oxygen surface diffusion [15], consistent with previous findings for the oxidation of pure copper [13]. Growth of the compact shape is due to efficient diffusion of adatoms on the metal surface and along island edges [16,17]. As oxidation progresses, a nonuniform partition of Au atoms develops in the alloy, and the local growth rate of the boundary adjacent to the Au-rich regions is slowed due to depletion of Cu atoms. As a result, the rate-limiting factor in these regions becomes Cu diffusion through the Au-rich zone, similar to reported behavior for oxidation of bulk Cu-Au alloys [11]. However, the growth of the dendritic tips is still controlled by fast oxygen surface diffusion because of the low Au accumulation in front of the tips. Therefore, boundary growth along the island perimeter has different rate-limiting factors that depend on the local concentration of Au in the alloy. Figure 4 is the schematic diagram showing our proposed model of Au segregation-induced dendritic growth. According to this picture, increasingly ramified morphologies are predicted as the oxidation proceeds.

Dendritic growth is a rather common phenomenon that can have important effects on behavior. Typical examples of processes that produce dendrites include solidification [18], development of viscous fingers in 2-phase liquids [19], and electro-deposition [20]. It is usually believed that the formation of dendrites in these systems results from competition between capillarity and kinetic effects, i.e., the interplay between the nonlocal diffusion that favors growth along the steepest gradient of the diffusion field and the surface tension that favors flat interfaces with minimum surface area [21,22]. However, two-dimensional (2D) dendrites formed during vapor deposition at low temperature represent an exception, where adatom diffusivity is high on the substrate, but is sufficiently low along island edges [23]. 2D dendritic growth has been modeled by diffusion-limited aggregation (DLA), in which an adatom performs a random walk on substrate, but is captured by a growing aggregate upon any encounter [24].

The stabilized value of 1.87 observed for the fractal dimension of the dendritic oxide islands in this study is considerably larger than the fractal dimension of $D_f = 1.71$ predicted by DLA theory [24]. The reason for this difference may be that two-dimensional, isotropic DLA is too simplistic to describe the oxidation reaction, which

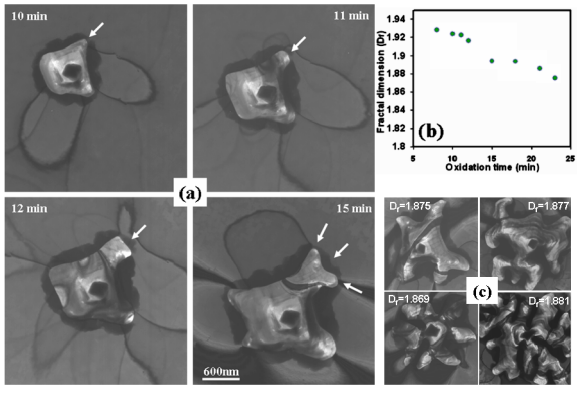

FIG. 3 (color online). (a) *In situ* observation of the tip splitting of an oxide island during the oxidation of Cu 15 at. % Au at 600 °C in $p(O_2) = 5 \times 10^{-4}$ Torr; (b) the fractal dimension of the oxide island is observed to decrease as a function of the oxidation time; (c) Oxide islands with several different dendritic morphologies have similar fractal dimensions.

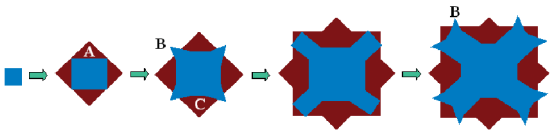

FIG. 4 (color). Schematics of the dendritic oxide growth in the oxidation of Cu-Au alloys; the label *A* denotes a Au-rich zone, *B* a region where growth is limited by oxygen surface diffusion, and *C* a region where growth is limited by Cu diffusion through a Au-rich zone.

involves diffusion and segregation of multiple species. For example, the accumulation of Au atoms in the alloy can change the sticking probability of oxygen onto the oxide-alloy interface by limiting the diffusion of Cu atoms through the Au-rich zone. The fractal dimension of 1.87 is also not compatible with the fractal dimension of ~ 1.5 associated with the dendrite formation in many other types of systems [18,25–27]. We expect that there exists a different, previously unobserved universal class to describe the segregation-induced dendritic oxide growth in the surface oxidation of two-component alloys containing only one oxidizing species.

Dendritic oxide formation was not observed at oxidation temperatures of 350–550 °C. We believe this is because the oxidation rate at these lower temperatures is slow, and within our observation time (usually less than 1 h) the oxide islands do not grow to the critical size associated with sufficient nonuniform Au buildup that leads to the change of the rate-limiting factors along the island perimeter. In contrast, at all oxidation temperatures ≥ 600 °C, dendritic oxide morphologies develop.

The stabilized fractal dimension of the dendrites, which depends on the oxide growth mechanism, does not show a change with increasing oxidation temperature above 600 °C. Increasing the oxidation temperature enhances the diffusion rates of both oxygen and copper, and as a result, increases the oxide growth rate; however, this does not change the mechanism that controls the formation of dendrites, i.e., the dependence of the local growth rate of the oxide on the composition of the alloy adjacent to the oxide islands. Similarly, the stabilized fractal dimension of the dendritic oxide shows no dependence on the oxygen partial pressure in the range of 1×10^{-4} to 8×10^{-4} Torr. However, we have observed that dendritic growth may be partially or completely suppressed by nucleating a very high number-density of oxide islands through greatly increasing either $p(O_2)$ (to approximately 10^{-2} Torr) or the Au mole fraction (to Cu 50% Au) in the original alloy [15]. The suppression of the transition to a dendritic morphology in these two cases occurs because islands begin to coalesce before reaching the critical size for the shape transition.

Island formation during oxidation has been observed for many pure metals, including Fe, Pd, Pb, Ti, Co, and Ni, as well as Cu [5,28–30], and dendritic oxide growth may also occur in the oxidation of alloy systems containing one reactive component such as Cu, Fe, Pd, etc., and one noble component such as Au or Pt, which do not form stable oxides under normal conditions. The dendritic transition causes a discontinuous morphology of the oxide, which is not desirable in many technological applications. In order to grow continuous, protective oxide films, it is necessary to nucleate a large number density of oxide islands, which will lead to full coalescence of the oxide islands prior to their dendritic transition. Therefore, this dendritic transition imposes a limitation on the oxidation conditions [i.e., high $p(O_2)$ is needed] to grow a continuous and protective oxide film. On the other hand, creation of complex patterns on surfaces is a fascinating area of interest in many fields. Our results suggest a new approach to growing dendritic oxide patterns on metal surfaces.

Argonne National Laboratory's work was supported by the U.S. Department of Energy, Office of Science, Office of Basic Energy Sciences, under Contract No. W-31-109-Eng-38. We thank R. Twesten, M. Marshall, and K. Colravy for their help in using the *in situ* TEM facility in the Materials Research Laboratory, University of Illinois at Urbana-Champaign.

*To whom correspondence should be addressed.
Email address: jeastman@anl.gov

[1] G. R. Wallwork, Rep. Prog. Phys. **39**, 401 (1976).
[2] M. P. Brady, B. Gleeson, and I. G. Wright, JOM **52**, 16 (2000).
[3] K. R. Lawless, Rep. Prog. Phys. **37**, 231 (1974).
[4] J. A. Eastman *et al.*, Appl. Phys. Lett. **87**, 051914 (2005).
[5] K. Thurmer, E. Williams, and J. Reutt-Robey, Science **297**, 2033 (2002).
[6] P. H. Holloway and J. B. Hudson, Surf. Sci. **43**, 123 (1974).
[7] J. C. Yang, D. Evan, and L. Tropia, Appl. Phys. Lett. **81**, 241 (2002).
[8] M. L. McDonald, J. M. Gibson, and F. C. Unterwald, Rev. Sci. Instrum. **60**, 700 (1989).
[9] G. W. Zhou and J. C. Yang, Phys. Rev. Lett. **93**, 226101 (2004).
[10] G. W. Zhou and J. C. Yang, Phys. Rev. Lett. **89**, 106101 (2002).
[11] C. Wagner, J. Electrochem. Soc. **99**, 369 (1952).
[12] D. B. Butrymowicz, J. R. Manning, and M. E. Read, *INCRA Monograph V: The Metallurgy of Copper* (International Copper Research Association, Inc., Washington, DC, 1977).
[13] J. C. Yang *et al.*, Appl. Phys. Lett. **70**, 3522 (1997).
[14] T. Vicsek, *Fractal Growth Phenomena* (World Scientific, New Jersey, 1992).
[15] G.-W. Zhou *et al.* (to be published).
[16] M. Li and J. W. Evans, Phys. Rev. B **69**, 035410 (2004).
[17] R. Q. Hwang *et al.*, Phys. Rev. Lett. **67**, 3279 (1991).
[18] U. Bisang and J. H. Bilgram, Phys. Rev. E **54**, 5309 (1996).
[19] R. Almgren, W. S. Dai, and V. Hakim, Phys. Rev. Lett. **71**, 3461 (1993).
[20] D. Barkey, F. Oberholtzer, and Q. Wu, Phys. Rev. Lett. **75**, 2980 (1995).
[21] T. C. Halsey, Phys. Today **53**, No. 11, 36 (2000).
[22] T. Vicsek, Phys. Rev. Lett. **53**, 2281 (1984).
[23] H. Roder *et al.*, Nature (London) **366**, 141 (1993).
[24] T. A. Witten and L. M. Sander, Phys. Rev. Lett. **47**, 1400 (1981).
[25] A. Arneodo *et al.*, Phys. Rev. Lett. **66**, 2332 (1991).
[26] E. Brener, H. Muller-Krumbhaar, and D. Temkin, Europhys. Lett. **17**, 535 (1992).
[27] J. Nittmann and H. E. Stanley, J. Phys. A **20**, L981 (1987).
[28] E. E. Hajcsar, P. R. Underhill, and W. W. Smeltzer, Langmuir **11**, 4862 (1995).
[29] S. Aggarwal *et al.*, Science **287**, 2235 (2000).
[30] D. F. Mitchell and M. J. Graham, Surf. Sci. **114**, 546 (1982).